



DISPLACEMENT-BASED DESIGN OF FACE-LOADED URM WALLS

Mike GRIFFITH¹, Nelson LAM², John WILSON³

SUMMARY

The displacement-based design (DBD) method has been previously shown to be an effective technique for the design of walls in vertical one-way bending subject to earthquake support motion. However, the accuracy of the technique has not been confirmed for support motions typical of that in the upper stories of low to mid-rise construction including unreinforced masonry (URM) construction. In these situations, the earthquake ground motion can be substantially “filtered” and amplified by the structure so that the conclusions from previous work considering only earthquake support motion cannot be automatically assumed to apply in this case. In this paper, the previously developed DBD procedure for the seismic assessment of URM walls is refined to account for the response behaviour of the URM building. The filtering effects in an URM building are first determined in accordance with the in-plane force-displacement properties of the supporting walls. The filtered excitations transmitted to the upper floors in the building are then used for analysing the wall face-loaded (out-of-plane) behaviour.

INTRODUCTION

Widespread failure of unreinforced masonry walls (URM) in a mere magnitude 5.6 earthquake in Newcastle, Australia in 1989 prompted intensive research for over a decade into the ultimate behaviour of URM walls under earthquake conditions. Predominant weak links that have been identified in typical URM construction are: (i) connections between floors and the supporting URM walls, and (ii) the out-of-plane bending actions of URM walls (Doherty *et al*, 1998). The first weak link could be addressed effectively in design by ensuring a minimum connection strength expressed in terms of force per unit length of the wall. Of particular concern is connections involving the use of DPC membranes. A design friction factor of 0.3 for such connections is considered reasonable (Doherty *et al*, 1998; Page, 1995). The connection strength capacity calculated with this assumption was found by Klopp and Griffith (1998) to be comparable to the typical strength demand predicted in accordance with the current Australian Earthquake Loading Standard (AS1170.4, 1993).

The importance of the second weak link was well demonstrated in the wall failure patterns observed in the Newcastle earthquake (Melchers, 1990), and is the focus of interests in this paper. The representation of the wall out-of-plane dynamic behaviour by the consideration of stresses and static equilibrium in

¹ Assoc. Professor, Dept. of Civil & Env. Eng., The University of Adelaide, AUSTRALIA

² Senior Lecturer, Dept. of Civil & Env. Eng., The University of Melbourne, AUSTRALIA

³ Assoc. Professor, Dept. of Civil & Env. Eng., The University of Melbourne, AUSTRALIA

conventional code procedures was found to be simplistic and inappropriate (Priestley, 1985). These important limitations with the conventional approach have also been confirmed by the authors through extensive experimental investigations (Griffith *et al*, 2004) in conjunction with analytical modeling (Lam *et al*, 2003). Results from these recent investigations have been used to develop an alternative, and a much more effective, displacement-based (DB) procedure which could provide realistic predictions for the out-of-plane behaviour of URM walls in an earthquake (Doherty *et al*, 2002).

In the proposed DB procedure, the kinematics of an URM wall is first generalised as a single-degree-of-freedom system in order that the out-of-plane equilibrium of the wall could be represented by a single force-displacement (F- Δ) relationship. Although such relationships appear highly non-linear (see *solid lines* in Figure 1) a dominant effective frequency, characteristics of linear elastic response behaviour, was observed from walls through impulse tests and earthquake simulations on the shaking table (Doherty *et al*, 2002). Consequently, reasonable predictions were obtained from analysis assuming a straight F- Δ line, the slope of which is the effective stiffness ($K_{s\text{-eff}}$) as shown by the *broken line* in Figure 1.

The F- Δ relationship for walls subject to low pre-compression (including parapet walls) is represented schematically by the *thin solid line* in Figure 1, based on the assumption of rigid-body behaviour. The wall effective stiffness ($K_{s\text{-eff}}$) is numerically equal to K_0 which is simply the threshold resistance for rocking (F_0) divided by the wall thickness (Δ_f). Expressions to obtain F_0 have been derived for walls with different boundary conditions based on statics (Doherty *et al*, 2002). Refer Figure 2 for examples.

Walls subject to high pre-compression are more complex and yet can be modelled by the tri-linear F- Δ relationship as shown by the *bold solid line* in Figure 1. The value for $K_{s\text{-eff}}$ is expressed as a function of both Δ_f and Δ_2 (see expression in Figure 1). Typical values for Δ_2 were found from racking tests to be in the range of 30- 50% of Δ_f , depending on the state of degradation of the wall; $K_{s\text{-eff}}$ is hence in the order of 1-2 K_0 .

Through linearisation, the wall displacement demand could be predicted in accordance with the elastic displacement response spectrum for any given “effective” natural period of the wall (T_{wall}). Since both $K_{s\text{-eff}}$ and the effective mass $M_{e\text{-ff}}$ (typically $\frac{3}{4}$ of the total mass of the wall) are now well defined, the fundamental period of rocking, T_{wall} , can be determined readily for any given boundary conditions, state of degradation and level of pre-compression commonly found in practice. A single-leaf wall is considered stable from out-of-plane overturning if the predicted maximum displacement demand is less than 50% of the displacement capacity, Δ_f (which is equal to the wall-thickness). This failure criterion is based on considering the position of the center of gravity of the wall in relation to its rocking edge.

The DB procedure summarized above is based on one-way vertical bending of the wall, and can be used to assess walls possessing high length-height aspect ratios or walls adjacent to large openings. In this paper, results obtained from further studies aimed at extending the procedure to account for two-way bending are presented. Displacement floor spectra were first obtained from dynamic analysis of linear elastic finite element models of 11 buildings located in Adelaide, South Australia using synthetic ground acceleration records that are consistent with design response spectra stipulated by the current Standard (AS1170.4, 1993). Four experimental F- Δ curves which account for two-way bending actions have been obtained to provide estimates for $K_{s\text{-eff}}$, and T_{wall} . The displacement demand (Δ_d) was obtained from the floor spectrum for each building, for comparison with the displacement capacity (Δ_{cap}). The performance index for each building based on the displacement ratio $\Delta_d/\Delta_{\text{cap}}$ is compared with similar indices based on conventional force-based calculation and dynamic analysis respectively. Comparisons between the performance indices reveal significant inconsistencies which point to drawbacks with the force-based procedure stipulated by current Standards.

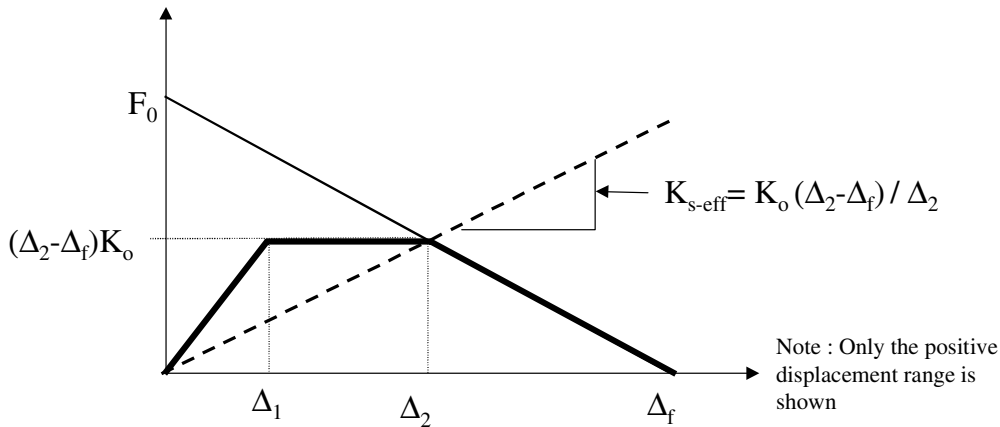
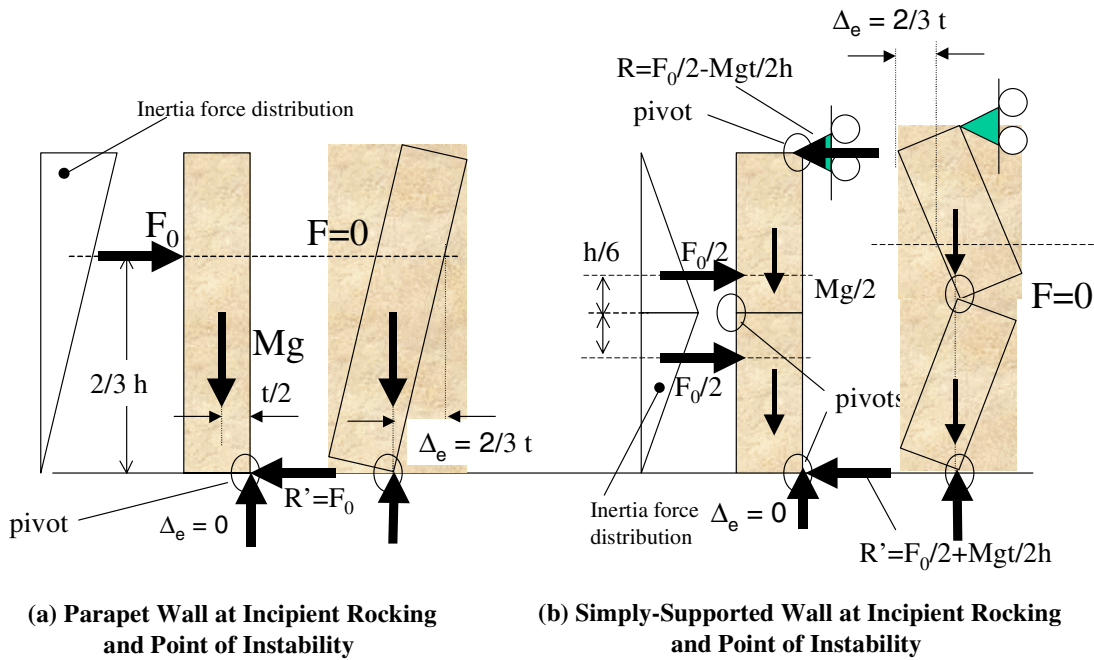


Figure 1. Definition of “effective stiffness”, $K_{s\text{-eff}}$.



(a) Parapet Wall at Incipient Rocking and Point of Instability

(b) Simply-Supported Wall at Incipient Rocking and Point of Instability

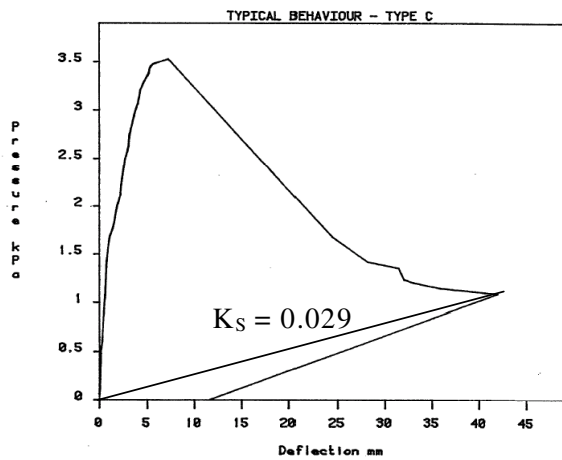
Figure 2. Definition of “effective displacement” Δ_e .

WALL LOAD-DEFLECTION CHARACTERISATION

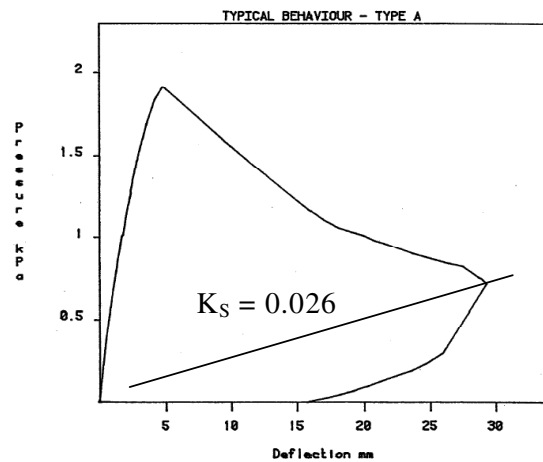
Lawrence (1983) and Griffith (2000) have conducted tests on laterally loaded brick masonry walls in two-way bending. Their results have been used to generalize what could be expected for typical values for the initial elastic stiffness and secant stiffness for possible use in the DBD method described earlier. The range of wall aspect ratios ($\alpha = L/H$) considered in Lawrence’s experimental work was $1 < \alpha < 2.4$ and the range of flexural tensile bond strength of the brickwork was $0.84 \text{ MPa} < f_{mt} < 2.31 \text{ MPa}$. Twelve of the 32 walls that Lawrence tested had similar boundary conditions to those tested by Griffith (2000). Lawrence characterized the typical load-deflection curve for brick masonry walls supported on three edges with the top edge free as that shown in Figure 3(b) and a wall supported on all four edges by the curve shown in Figure 3(a). It should be noted here that the point of maximum displacement on the load deflection curves in Figure 3 does not correspond to the point of wall collapse. As can be seen in Figure 3(a) the wall is still

able to support a sizeable lateral pressure at a displacement of 40mm (nearly half the wall thickness). The walls were unloaded at this point where it can be seen in all cases that the unloading path was different from the loading path, leaving the walls with some residual lateral deformation. The curves from Griffith's two tests are for a wall supported at all four edges with vertical precompression ($\sigma_v = 0.04 \text{ MPa}$) in Figure 3(c) and a wall supported at three edges with the top edge free in Figure 3(d). It was noted that while the precompression in the wall represented by Figure 3(c) enabled the wall to maintain its maximum strength for some time beyond its cracking displacement, this would not be expected to occur in walls near the top of buildings where the out-of-plane accelerations are typically largest and the precompression stresses at their minimum.

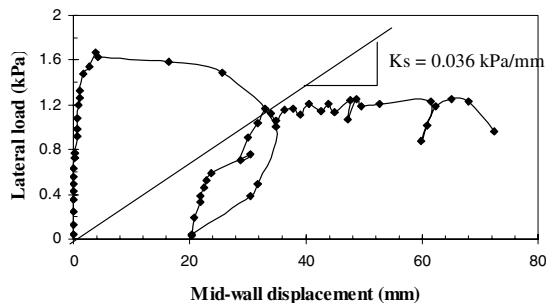
Of main interest here is the value of the secant stiffness, $K_{s\text{-eff}}$. Remarkably, the secant stiffness values for the walls represented in Figure 3 are all very similar, varying only between 0.026 kPa/mm and 0.036 kPa/mm . Hence, it was assumed for this exercise to use a constant value of $K_{s\text{-eff}} = 0.030 \text{ kPa/mm}$ to estimate the post-cracking vibrational period T_{wall} ($= 0.36$ seconds) for all the walls in the 11 URM buildings being considered. The reason that a single value of stiffness gives the same period for all 11 walls is because they also all had the same thickness ($t_u = 110 \text{ mm}$) and weight density ($\gamma = 18 \text{ kN/m}^3$).



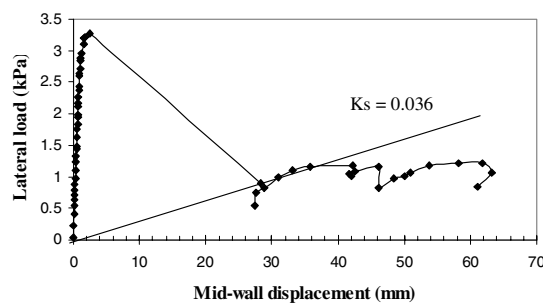
(a) Typical load-deflection curve for wall supported on all 4 sides (Lawrence, 1983).



(b) Typical load-deflection curve for wall with top edge free (Lawrence, 1983).



(c) Wall supported on 4 sides and 0.05MPa precompression (Griffith, 2000).



(d) Wall with top edge free and no precompression (Griffith 2000).

Figure 3 – Typical load versus deflection curves for laterally load brick masonry walls.

DESCRIPTION OF URM BUILDINGS IN CASE STUDIES

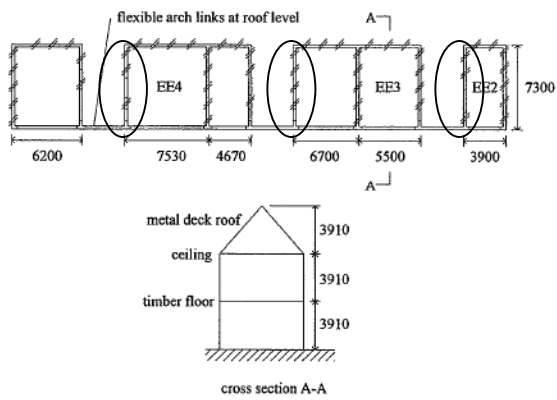
Eleven unreinforced brick masonry (URM) buildings previously studied by Klopp and Griffith (1993) were used as case studies in this project. The 11 buildings were all located in Adelaide, South Australia and range in height from 4.6m (2 stories) to 19.2m (6 stories). All buildings were constructed of clay brickwork using units with the nominal dimensions of 230mm x 110mm x 76mm (length/width/height) and 10mm thick mortar joints. The exterior walls in all buildings consisted of two leafs of 110mm thick brickwork separated by a 80mm gap. For the purposes of this analysis, it was assumed that the exterior leaves were well “tied” to the interior leaves in these “cavity” walls and that they shared the loads equally. The typical floor plans and elevations for each building are presented in Figure 4. Complete details of the buildings can be found in Klopp (1994).

For the purposes of the present work, one top-storey wall was considered from each building since the out-of-plane accelerations are normally greatest at the top of a building where the vertical compressive stresses and hence the out-of-plane flexural strength of a wall is at its minimum. The respective walls considered for each building are circled in Figure 4.

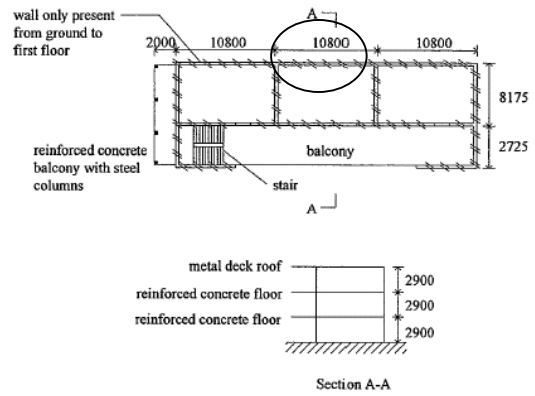
The strength of each wall was calculated in accordance with the expressions given in the Australian Masonry Structures Code, AS 3700 (SA, 2001) using typical material properties listed below in Table 1. These material properties were used in all associated calculations and structural modeling. It should be noted that “characteristic” values (i.e., mean value minus 1.65 standard deviations) were used to calculate the strength (capacity) of the URM walls whereas the actions of the loading (demand) were calculated using the design acceleration coefficient, acceleration spectrum, or 12-second ground motion time history corresponding to the 500-year return period earthquake.

Table 1. Material properties used in calculation of wall design strength, w_{cap} .

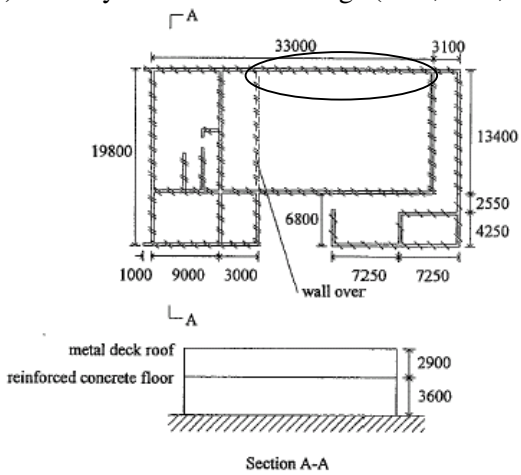
Property	Variable and value
brick unit length	$l_u = 230 \text{ mm}$
brick unit width (wall thickness)	$t_u = 110 \text{ mm}$
brick unit height	$h_u = 76 \text{ mm}$
mortar joint thickness	$t_j = 10 \text{ mm}$
flexural tensile strength of brick-mortar bond	$f_{mt} = 0.20 \text{ MPa}$
flexural tensile capacity of brick units	$f_t = 1.0 \text{ MPa}$
Young’s modulus for brickwork	$E = 1100 \text{ MPa}$
weight density of brickwork	$\gamma = 18 \text{ kN/m}^3$
capacity reduction factor for flexural design	$\phi = 0.6$



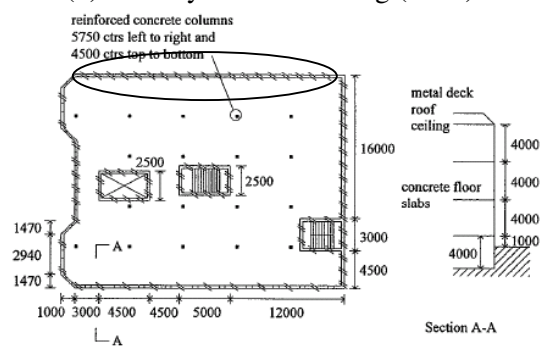
(a) 2-storey warehouse buildings (EE2, EE3, EE4)



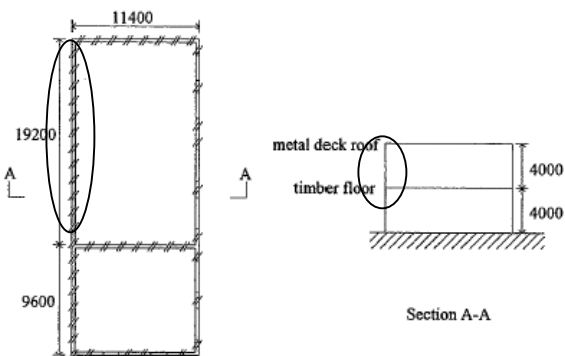
(b) 3-storey school building (CBC)



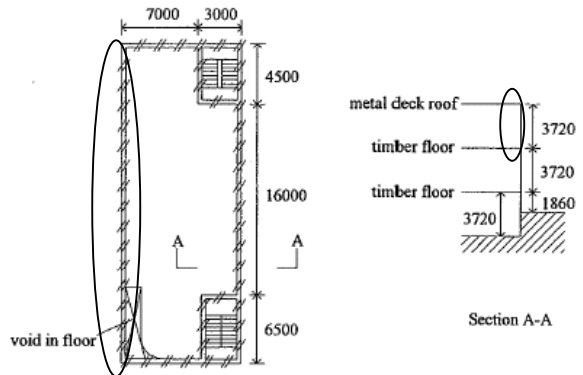
(c) 2-storey commercial building (IAC)



(d) 4-storey office building (LTI)



(e) 2-storey warehouse building (NSC)



(f) 3-storey bookstore (STP)

Figure 4. Building plan and elevation details (continued next page).

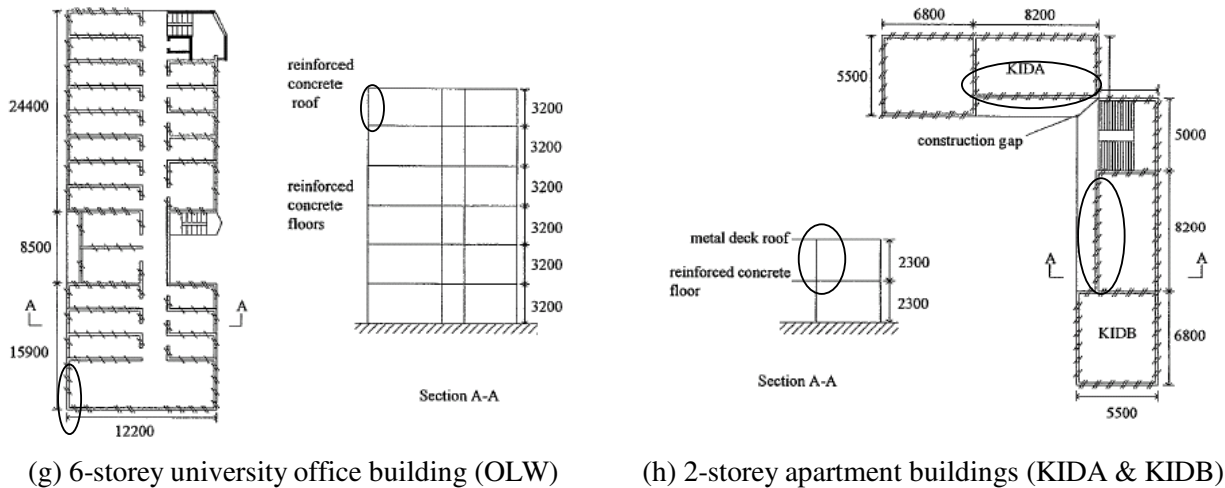


Figure 4 (continued). Building plan and elevation details.

The calculated periods for each of the 11 buildings are listed in Table 2. The ratio of the building period, T_{bldg} , to the effective rocking period for a URM wall, T_{wall} , determines to a large extent how much the floor vibrations are amplified in a wall's rocking vibration since the dominant vibration frequencies in the floor motion will correspond closely to the dominant building vibration frequencies. As can be seen in Table 2, only the LTI and OLW buildings have building-period to wall-period ratios approaching 1 (i.e., 0.69 and 0.83 respectively). Not surprisingly, these are also the two tallest buildings in this study. It will be seen subsequently that the walls at the top of those two buildings are the only two walls to have correspondingly large displacement demands calculated from the floor displacement spectra.

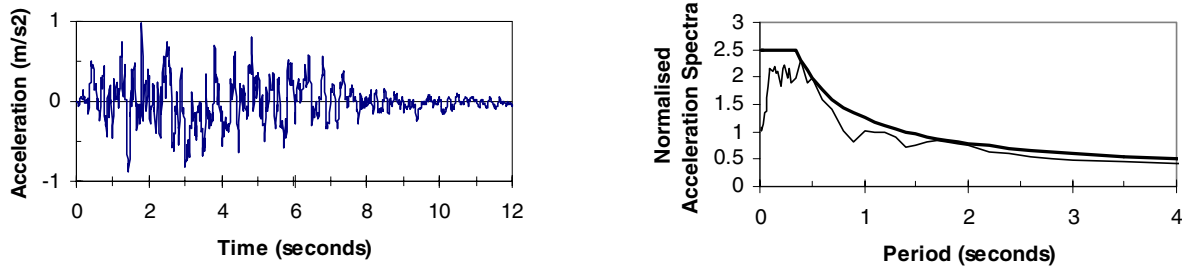
Table 2. Calculated building periods and ratio to wall period T_{wall} .

Building	Period, T_{bldg} (seconds)	$\frac{T_{bldg}}{T_{wall}}$
CBC	0.18	0.50
EE2	0.17	0.47
EE3	0.11	0.31
EE4	0.11	0.31
IAC	0.15	0.42
KIDA	0.09	0.25
KIDB	0.08	0.22
LTI	0.25	0.69
NSC	0.14	0.39
OLW	0.30	0.83
STP	0.20	0.56

GROUND MOTION AND FLOOR SPECTRA

The 12 second ground motion used to excite the 11 buildings in this study is shown in Figure 5(a) and was derived from the 5% damped design acceleration spectrum specified in the Australian earthquake loading code (SA, 1993). As shown in Figure 5(b), the 5% damped acceleration response spectra for the "code-compatible" ground motion agrees reasonably well with the design spectra for periods greater than 0.5

seconds and only underestimates the design curve by about 20% for periods less than 0.5 seconds which is the typical range for low-to-medium rise masonry buildings.

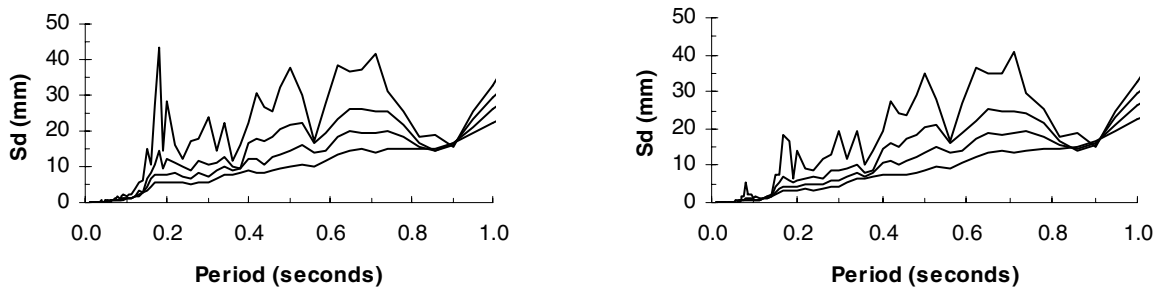


(a) Code compatible ground motion record

(b) Ground motion and design spectra

Figure 5. Ground motion time history and acceleration spectra used for analyses.

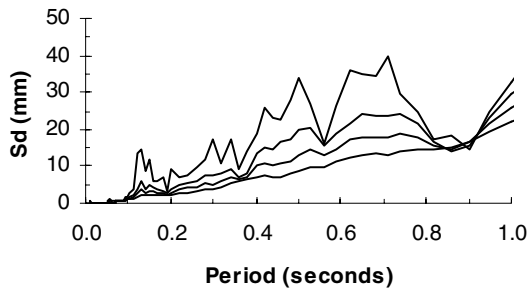
The corresponding 5% damped floor spectra were calculated for each building from the horizontal acceleration time history response for the top storey floor in each building. It can be seen that the first peak (going from left to right in Figure 6) in the floor displacement spectra for each of the 11 buildings corresponds to each buildings' first natural period, T_{bdg} , of vibration listed in Table 2. Where the spikes in the displacement spectra coincide with the rocking period for a URM wall, T_{wall} , there will be a significant amplification of the floor displacement in the wall response. However, where the spike occurs at a frequency significantly removed from the rocking period for a wall there will be very little amplification in the wall displacements. In that case, the maximum wall displacement will not be much different than that given by the displacement spectra for the ground motion instead of the actual floor motion. For example, the 5% damped displacement spectra value at $T_{\text{wall}} = 0.36$ seconds for the ground motion (Figure 6(l)) is about 5mm while the 5% damped displacement spectrum value at $T_{\text{wall}} = 0.36$ seconds for the 1st floor motion in the CBC building (Figure 6(a)) is about 7mm, an amplification of 40%. In contrast, the 5% damped displacement spectrum value at $T_{\text{wall}} = 0.36$ seconds for the 6th floor motion in the OLW building is about 30mm, an amplification of 600%.



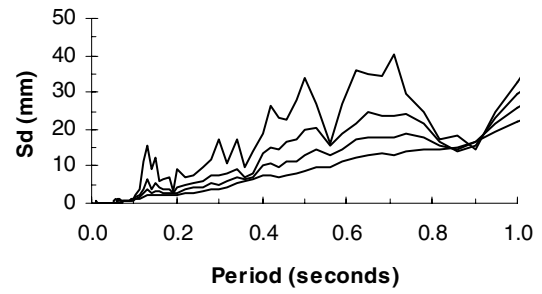
(a) CBC building – 1st floor spectra
(0, 2, 5, and 10% damping)

(b) EE2 building – 2nd floor spectra
(0, 2, 5, and 10% damping)

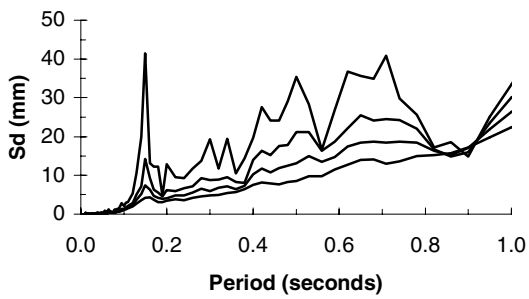
Figure 6. Displacement spectra for top storey in buildings subject to code-compatible earthquake ground motion (continued next page).



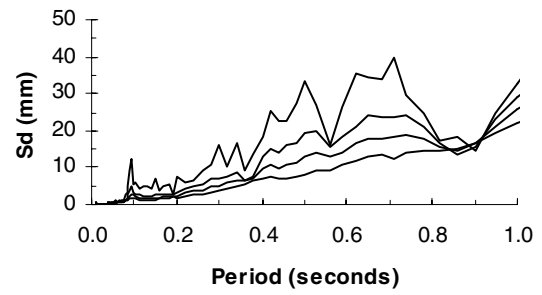
(c) EE3 building – 2nd floor spectra
(0, 2, 5, and 10% damping)



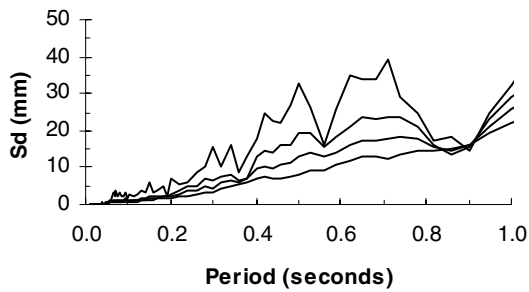
(d) EE4 building – 2nd floor spectra
(0, 2, 5, and 10% damping)



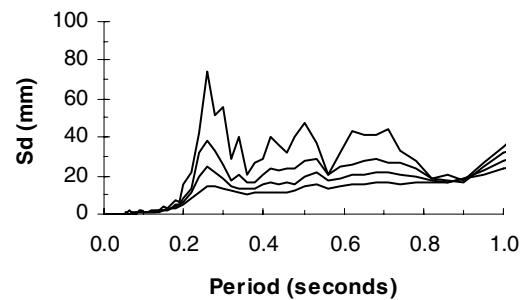
(e) IAC building – 1st floor spectra
(0, 2, 5, and 10% damping)



(f) KIDA building – 2nd floor spectra
(0, 2, 5, and 10% damping)

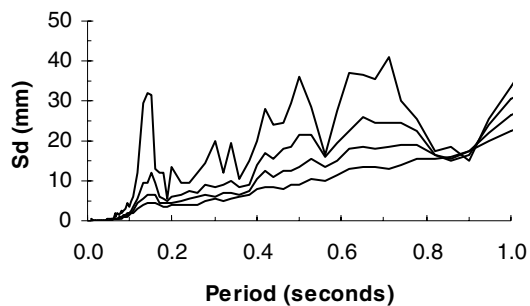


(g) KIDB building – 1st floor spectra
(0, 2, 5, and 10% damping)

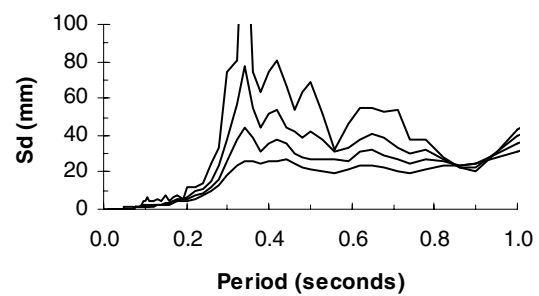


(h) LTI building – 2nd floor spectra
(0, 2, 5, and 10% damping)

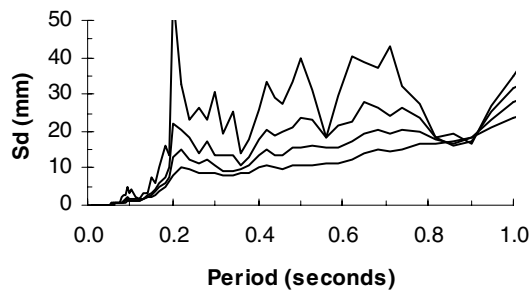
Figure 6 (continued). Displacement spectra for top storey in buildings subject to code-compatible earthquake ground motion (continued next page).



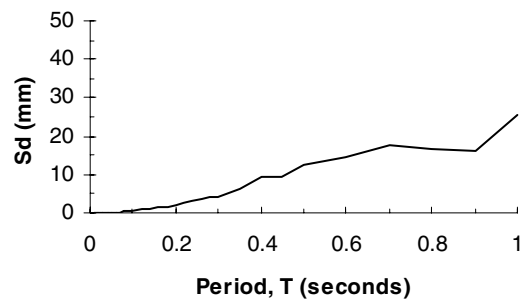
(i) NSC building – 2nd floor spectra
(0, 2, 5, and 10% damping)



(j) OLW building – 5th floor spectra
(0, 2, 5, and 10% damping)



(k) STP building – 2nd floor spectra
(0, 2, 5, and 10% damping)



(l) displacement spectra for ground motion
(5% damping)

Figure 6 (continued). Displacement spectra for top storey in buildings subject to code-compatible earthquake ground motion.

RESULTS OF ANALYSES AND DISCUSSION

The results of the elastic force-based static analyses are listed in columns 2 – 4 of Table 3 for each of the 11 buildings considered. The corresponding results of the elastic dynamic (response spectrum) analyses and the displacement-based analyses are listed in columns 5-7 and 8-10 of Table 3, respectively. They are discussed in turn in the following sections.

Force-based Static Analyses

The static force-based calculations for load, F_p , were calculated using Section 5 of the Australian Earthquake Loading Standard which follows the UBC approach for calculating forces on parts (architectural components) of buildings and are listed in column 2 of Table 3. The wall capacity values, w_{cap} , were calculated using the expressions in the Australian Masonry Structures code AS 3700 and are listed in column 3 of Table 3.

In this analysis, failure is deemed to occur when the ratio of F_p/w_{cap} (column 4 of Table 3) is greater than 1. On this basis, failure was predicted to occur in 8 out of 11 walls using this equivalent static “Force-Based” method of analysis. Walls in KIDA, KIDB, and OLW did not fail due to their low aspect ratio, low height and especially their relatively short wall span. Walls in the STP, LTI, NSC and IAC buildings were all predicted to fail badly due to their large aspect ratio and long wall spans.

Dynamic Analyses

The results of the dynamic analysis in Table 3 are taken from the study by Klopp and Griffith (1998), where each building was subjected to a linear elastic response spectrum analysis using the 5% damped acceleration spectrum for design given in AS 1170.4 shown in Figure 5(b). The values for σ_b are the maximum principal bending stresses calculated in the vertical direction and are listed in column 5 of Table 3. They are compared to the nominal minimum flexural bending strength of the brickwork, $f_{mt} = 0.2MPa$ with “failure” defined to occur when the ratio of σ_b/f_{mt} is greater than 1 (column 7 of Table 3).

As can be seen, the dynamic analysis results are reasonably consistent with the results of the force-based static analyses except that here the OLW wall is also predicted to fail due to the fact that the dynamic analysis predicted significant building/wall resonance in the OLW building, leading to significant amplifications in the wall response above that in the floor (refer to Figure 6(j)).

Displacement-based Analyses

The values of T_{wall} listed in Table 2 were used along with the floor spectra shown in Figure 6 to calculate the corresponding spectral displacement for walls in each of the 11 URM buildings. As noted earlier, the spectral displacements (Δ_{eff}) were multiplied by 1.5 to obtain estimates of the maximum wall displacements, Δ_d , expected to occur in buildings subjected to the code compatible ground motion. These values are given in column 8 of Table 3. The displacement capacity for each wall was assumed, for this exercise, to be half the wall thickness which was 55mm for all walls. Observing the ratio of the predicted maximum displacements to the capacity of 55mm in column 10 of Table 3 indicates that only the walls in the 5th floor of the OLW building are likely to fail. However, it should be noted that the assumption of 55mm for the wall capacity was somewhat arbitrary given that walls tend not to collapse under displacement-control loading until displacements approaching the full wall thickness are reached.

Table 3. Results of force- and displacement-based analyses for walls in case study.

Building	Force-based Static Analysis			Dynamic Analysis			Displacement-based Analysis		
	F_p (kPa)	w_{cap} (kPa)	$\frac{F_p}{w_{cap}}$	σ_b (MPa)	f_{mt} (MPa)	$\frac{\sigma_b}{f_{mt}}$	Δ_d (mm)	Δ_{cap} (mm)	$\frac{\Delta_d}{\Delta_{cap}}$
CBC	0.65	0.327	1.65	0.25	0.20	1.25	13.0	55.0	0.24
EE2	0.62	0.418	1.23	0.20	0.20	1.00	10.65	55.0	0.19
EE3	0.62	0.418	1.23	0.20	0.20	1.00	9.60	55.0	0.17
EE4	0.62	0.401	1.28	0.20	0.20	1.00	9.60	55.0	0.17
IAC	0.63	0.157	3.32	0.30	0.20	1.50	9.60	55.0	0.17
KIDA	0.62	0.546	0.94	0.15	0.20	0.75	9.30	55.0	0.17
KIDB	0.62	0.546	0.94	0.15	0.20	0.75	9.00	55.0	0.16
LTI	0.66	0.083	6.57	1.4	0.20	7.00	19.80	55.0	0.36
NSC	0.62	0.129	3.98	0.52	0.20	2.60	9.90	55.0	0.18
OLW	0.68	0.621	0.91	0.75	0.20	3.75	58.8	55.0	1.07
STP	0.64	0.095	5.54	0.51	0.20	2.55	9.15	55.0	0.26

SUMMARY AND CONCLUDING REMARKS

The use of displacement-based analysis to assess the seismic capacity of unreinforced brick masonry walls in 2-way bending has been compared to the current static force-based method specified in earthquake codes for “parts of buildings” and to the response spectrum (“dynamic”) analysis method. Walls in eleven buildings were considered as case studies to investigate the strengths and weaknesses of the various methods.

The elastic force based (FB) analyses and dynamic analyses (DA) both predicted most walls would crack and fail due to the flexural tensile strength of the masonry (f_{mt}) being exceeded. The dynamic analyses suggested that walls with natural frequencies near that of the building (LT1 and OLW, refer Table 2 and Figs 4h and 4j) would be subject to resonance and a significant amplification in response and bending stresses. The static FB analyses indicated that the walls with a large aspect ratio (α) and large design length (L_d) (IAC, LT1, NSC, STP) had a lower inherent resistance to out-of-plane loads and hence were more susceptible to earthquake excitation. In contrast, the displacement based (DB) analyses indicated that only one wall (OLW) developed sufficient out-of-plane displacement to cause wall instability and failure.

These analyses indicated that the elastic analyses are useful for investigating the onset of cracking (ie. bending stress demand exceeds capacity) but they are poor predictors of failure (defined here to be collapse). Cracking induced under earthquake excitation indicates the formation of a mechanism which must be checked using DB procedures to assess overall wall stability. Interestingly in these case study examples, the elastic analyses indicated that between 8 and 9 walls would fail compared with the DB procedure which indicated that only one wall was marginal and in danger of failure.

Of course, the use of an effective secant stiffness to represent non-linear, inelastic response of walls in 2-way bending needs to be validated as was done by the authors previously for walls in 1-way vertical bending. Questions that must be answered also include whether a constant damping value is appropriate. If so, what value? If not, how can variable (hysteretic) damping be accounted for? This work is ongoing.

REFERENCES

1. Melchers RE (ed.). *Newcastle Earthquake Study*. The Institution of Engineers, Australia, 1990.
2. Page AW. "Unreinforced masonry structures – an Australian Overview, *Fifth Pacific Conference on Earthquake Engineering*, University of Melbourne, 1-16, 1995.
3. Doherty K, Lam NTK, Griffith M and Wilson JL. "Investigation of the Weak links in the seismic load path of unreinforced masonry buildings", *Proceedings of the 5th Australasian Masonry Conference*, 1-3 July, 1998.
4. Lam, N., Griffith, M., Wilson, J. and Doherty, K. "Time History Analysis of URM walls in out-of-plane flexure", *Journal of Engineering Structures*. Elsevier Science Publisher. Vol.25(6):743-754, 2003.
5. Griffith, M., Lam, N., Wilson, J. and Doherty, K. "Experimental Investigation of Unreinforced Masonry Walls in Flexure", *Journal of Structural Engineering*, The American Society for Civil Engineers. Vol.130(3), 2004.
6. Klopp, G.M., Griffith, M.C. "Seismic analysis of unreinforced masonry buildings," *Australian Journal of Structural Engineering*, Vol. SE1(2): 121 – 131, 1998.
7. Klopp, G.M., Griffith, M.C. "Dynamic characteristics of unreinforced masonry buildings," *Australian Civil Engineering Transactions*, Vol. CE35(1): 59 – 68, 1993.
8. Doherty, K., Griffith, M.C., Lam, N.T.K., Wilson, J.L. "Displacement-based analysis for out-of-plane bending of seismically loaded unreinforced masonry walls," *Earthquake Engineering and Structural Dynamics*, Vol. 31(4): 833-850, 2002.
9. Lawrence, S.J. "Behaviour of brick masonry walls under lateral loading," PhD thesis, School of Civil Engineering, The University of New South Wales, Australia, 1983.
10. Standards Australia, 2001. "Masonry Structures," Australian Standard AS 3700, Standards Australia, Homebush, NSW.

11. Standards Australia, 1993. "Minimum design loads on structures, Part 4: Earthquake Loads," Australian Standard AS1170.4, Standards Australia, Homebush, NSW.
12. Priestley, M.J.N. "Seismic behaviour of unreinforced masonry walls," *Bulletin of the New Zealand Society for Earthquake Engineering*, Vol. 18(2), 191 – 205, 1985.
13. ABK
14. Griffith, M.C., 2000. "Experimental study of the flexural strength of URM (Brick) walls," Research Report No. R169, Department of Civil and Environmental Engineering, The University of Adelaide, 21p.